Fock-space WKB method for the boson Josephson model describing a Bose-Einstein condensate trapped in a double-well potential

V. S. Shchesnovich[1] and M. Trippenbach[2]
[1]*Universidade Federal do ABC, Centro de Ciências Naturais e Humanas, Rua Santa Adélia, 166, 09210-170, Santo André, Brazil*
[2]*Institute of Experimental Physics, Optics Division, Warsaw University, ul. Hoża 69, Warsaw 00-681, Poland*
(Received 1 April 2008; revised manuscript received 1 June 2008; published 6 August 2008)

We develop a Fock-space WKB method for a Bose-Einstein condensate (BEC) in a double-well trap, using an analogy with a single particle of either positive or negative mass in a quantum potential. The usual mean-field approach is the classical limit, and the inverse number of atoms plays the role of Planck constant. The ground state of positive-mass particles corresponds to the mean-field fixed point of lower energy, while that of negative mass to the excited fixed point. In the case of attractive BECs above the threshold for symmetry breaking, the ground state is the Schrödinger cat state and we relate this to the double-well shape of the potential in Fock space. In the repulsive case, we identify the quantum states corresponding to the mean-field macroscopic self-trapping phenomenon. In particular, the phase-locked (π phase) macroscopic quantum self-trapping of BECs is related to the double-well shape of the potential in Fock space. The running-phase macroscopic quantum self-trapping state is found to be subject to quantum collapses and revivals. The phase dispersion grows exponentially, reaching the absolute maximum just before the first collapse of the running phase, which may explain the growth of the phase fluctuations seen in the experiment on macroscopic quantum self-trapping.

DOI: 10.1103/PhysRevA.78.023611 PACS number(s): 03.75.Lm, 03.75.Nt

I. INTRODUCTION

The analytical description of a system of a large number N of interacting bosons is a difficult problem. In the case of Bose-Einstein condensate (BEC), characterized by a macroscopic number of atoms, $N \gg 1$, the usual approach is the mean-field substitution of the boson field operators by scalars, which leads to the Gross-Pitaevskii equation [1–3]. The relation between the full quantum and mean-field dynamics of BEC is a subject of intensive studies. Of particular interest are the classical bifurcation and its significance for the quantum spectrum [4], quantum collapses and revivals [5], the many-body quantum corrections to the mean-field theory [6,7] (decoherence), and the correspondence between the many-body quantum and classical dynamics in phase space [8]. Recently, in a study of the nonlinear two- and three-mode boson models describing BEC interband tunneling in optical lattices [9,10], it was found that the quantum evolution distinguishes between stable and unstable mean-field fixed points, following the classical dynamics about the stable points and diverging from it at the unstable ones. One of the insights of these studies was a link between the WKB approach for the discrete Schrödinger equation (see, for instance, Ref. [11]) and the large boson limit of the few-mode boson models.

The purpose of this paper is to study in more detail the analytical method for boson systems based on an analogy with the discrete WKB approach. Our approach is based on the fact that for $N \gg 1$ the s-mode boson model is equivalent to a quantum mechanical dynamics of a single particle residing in a compact $(s-1)$-dimensional space. We consider the important two-mode model describing BEC in a double-well potential—i.e., the boson Josephson junction (see, for instance, the reviews in [12,13]). This system is a subject of fundamental experiments and has many potential applications; it was already used for observation of macroscopic quantum tunneling and macroscopic self-trapping [14], whereas future proposals include also the atomic Mach-Zehnder interferometer [15,16], the sensitive weak force detector [17,18], and the atomic interferometer on a chip [19]. The two-mode boson model is analogous to a nonrigid quantum pendulum if one uses the phase quantization method. For instance, this method was previously used to study the thermal versus quantum decoherence [20]. The exact quantum Hamiltonian for the model in phase space has been derived in Ref. [21].

We work in Fock space and study the relation between the mean-field fixed points, the most important features of the classical dynamics, and the corresponding quantum states. In particular, we point out that there are two different Schrödinger equations for a description of quantum dynamics, corresponding to positive and negative mass of the effective quantum particle in Fock space. The approach allows us to identify the quantum states corresponding to the mean-field phase-locked (π phase) macroscopic self-trapping phenomenon [22] as bound states of the negative-mass quantum particle. We also show that the experimentally observed running-phase macroscopic self-trapping [14] is subject to quantum collapse of the running phase. For a small number of atoms, the sequence of collapses and revivals is observed. A rapid exponential growth of the quantum phase dispersion precedes the quantum collapse of the running phase.

The paper is organized as follows. In Sec. II we derive the effective particle representation of the quantum-boson Josephson-junction model. The two reduced Schrödinger equations for the effective quantum particle are studied in Sec. III. In Sec. IV we study the ground state of the quantum model. In Sec. V the macroscopic quantum self-trapping (MQST) phenomenon is related to the negative-mass effective quantum particle. We also study the quantum dynamics

of the experimentally observed running-phase MQST. Section VI contains a discussion of the main results.

II. QUANTUM PARTICLE APPROACH FOR BEC IN A DOUBLE-WELL TRAP

We consider the case of sufficiently weak atomic interaction, when only the degenerate energy levels of the double-well trap are occupied by BEC (more precisely, when the first two energy levels are quasidegenerate, $\delta E = E_2 - E_1 \ll E_3 - E_2 = \Delta E$). The reduced Schrödinger equation for the system reads (see, for instance, Refs. [8,13,23] and Appendix A)

$$\frac{i}{N}\partial_\tau |\psi\rangle = \hat{H}|\psi\rangle,$$

$$\hat{H} \equiv \left\{ -\frac{1}{N}(a_1^\dagger a_2 + a_2^\dagger a_1) + \frac{\varepsilon}{N} n_1 + \frac{\gamma}{N^2}(n_1^2 + n_2^2) \right\}, \qquad (1)$$

where $|\psi\rangle$ is the system state, $n_j = a_j^\dagger a_j$ [the boson field operator is expanded over the localized states $\Psi = \varphi_L(\mathbf{x})a_1 + \varphi_R(\mathbf{x})a_2$], and the time is measured in tunneling time units: $\tau = t/T$. The parameters of the model are defined as

$$T = \frac{2\hbar}{\delta E}, \quad \varepsilon = \frac{2\delta V}{\delta E}, \quad \gamma = \frac{gN}{\delta E}\int d^3\mathbf{x}\varphi_{L,R}^4,$$

$$\delta E = -2\int d^3\mathbf{x}\varphi_L\left(-\frac{\hbar^2}{2m}\nabla^2 + V(\mathbf{x})\right)\varphi_R,$$

$$\delta V = \int d^3\mathbf{x}[\varphi_L V(\mathbf{x})\varphi_L - \varphi_R V(\mathbf{x})\varphi_R], \qquad (2)$$

where $g = 4\pi\hbar^2 a_s/m$ with a_s being the s-wave scattering length, $V(\mathbf{x})$ is the double-well potential in one of the coordinates (centered at zero, for below), and the localized states $\varphi_L(\mathbf{x})$ and $\varphi_R(\mathbf{x})$ are given by the normalized sum and difference of the ground state and the first excited state of the "symmetrized" double-well potential $V_s(\mathbf{x}) \equiv [V(\mathbf{x}) + V(-\mathbf{x})]/2$ (for more details, see the Appendix in Ref. [24]; due to the symmetry, the integrals of the fourth power are equal).

Note that δV can be of the same order as δE; thus, ε is arbitrary and γ is finite (not small), while the applicability condition that the interaction energy be much less than the average trap energy spacing—i.e., $\gamma \ll \Delta E/\delta E$—is satisfied due to the large right-hand side (rhs).

Subtracting the quantity $\frac{\gamma}{2N^2}(n_1+n_2)^2 = \frac{\gamma}{2}$, due to the total number of atoms conservation $N = n_1 + n_2$, from the Hamiltonian in Eq. (1) we obtain the standard representation of the Hamiltonian for the boson Josephson junction. Our interaction parameter is related to the standard parameters as follows: $\gamma = E_c N^2/E_j$ (we also note that $\gamma = \Lambda$ of Refs. [14,22]).

We have divided the Schrödinger equation (1) by N and defined the parameters by extracting the explicit N factors reflecting the "order" of the respective boson operators (e.g., $a_1^\dagger a_1 \sim N$). This allows us to introduce the effective quantum particle representation of Eq. (1) [see Eq. (5) below]. It is important to observe for the following that the physical parameters of the model are N independent in the thermodynamic limit, which is $N \to \infty$ at a constant density $\frac{N}{\mathcal{V}}$, where $\mathcal{V}$ is the volume occupied by the system. Indeed, T, δE, and ε are evidently independent of N, while the nonlinear parameter $\gamma \sim \frac{gN}{\delta E \mathcal{V}}$ since $|\varphi_\alpha|^4 \sim \mathcal{V}^{-2}$.

On the other hand, the extra factor N^{-1} on the lhs of Eq. (1) can be considered as an effective Planck constant; hence, the thermodynamic limit $N \to \infty$ is also the semiclassical limit. To make this clearer, let us rewrite Eq. (1) in the explicit form using the Fock basis

$$|\psi\rangle = \sum_{k=0}^{N} C_k |k, N-k\rangle, \qquad (3)$$

where the occupation number corresponding to the left well is denoted by k. We get

$$\frac{i}{N}\frac{d}{d\tau}C_k = -(b_{k-1}C_{k-1} + b_k C_{k+1}) + a_k C_k, \qquad (4)$$

with

$$b_k = N^{-1}[(k+1)(N-k)]^{1/2},$$

$$a_k = \gamma N^{-2}[k^2 + (N-k)^2] + \varepsilon N^{-1}k.$$

Introducing the continuous variable $x = k/N$, the analog of the Planck constant $h = 1/N$ and a wave function $\Psi(x) = \sqrt{N}C_k$ we obtain Eq. (1) in the continuous-variable representation

$$ih\partial_\tau \Psi(x) = -\{e^{-i\hat{p}}b_h(x) + b_h(x)e^{i\hat{p}}\}\Psi(x) + a(x)\Psi(x), \quad (5)$$

with $\hat{p} = -ih\partial_x$ and

$$b_h(x) = [(x+h)(1-x)]^{1/2}, \quad a(x) = \gamma[x^2 + (1-x)^2] + \varepsilon x.$$

Here $x \in (0,1)$ and $\hat{p} \in (0, 2\pi)$ are canonical variables, with $[\hat{p}, x] = -ih$.[1] Note that the inner product for $N \gg 1$ reads $\langle \Psi_1 | \Psi_2 \rangle = \int_0^1 dx \Psi_1^*(x)\Psi_2(x)$.

It is instructive to rewrite Eq. (5) in the phase quantization representation by putting $\hat{p} \to \phi$ and $x - 1/2 \to ih\partial_\phi$ (the shifted variable is more convenient). In a more rigorous way, one can use the transformation of the state vector C_k to the Fourier space, given in our case by the discrete Fourier transform (see also Refs. [25]),

$$C_k = \frac{1}{\sqrt{N+1}}\sum_{l=0}^{N} e^{-ik\phi_l}\tilde{C}_l, \quad \tilde{C}_l = \frac{1}{\sqrt{N+1}}\sum_{k=0}^{N} e^{ik\phi_l}C_k, \qquad (6)$$

where $\phi_l = 2\pi l/(N+1)$. Using periodicity of the exponent we have for $N \gg 1$

[1] The wave function $\Psi(x)$ is supposed to decay to zero at the boundaries of the interval [0,1], as is in all the cases in this paper. The difficulties with defining the conjugated phase and amplitude variables in the quantum case are well known; see, for instance, Ref. [35].

$$\Psi(x)=\frac{1}{2\pi}\int_{-\pi}^{\pi}d\phi e^{iN\phi x}\tilde{\Psi}(\phi),\quad \tilde{\Psi}(\phi)=N\int_{0}^{1}dx e^{-iN\phi x}\Psi(x), \tag{7}$$

where $\tilde{\Psi}(\phi_l)=(N+1)\tilde{C}_l$. Thus, for $N\gg 1$ the Hamiltonian for the boson Josephson junction in the ϕ representation reads (save an inessential constant term)

$$\hat{H}=-2\gamma h^2\partial_\phi^2-\{b_h(1/2+ih\partial_\phi),\cos(\phi)\}+i\varepsilon h\partial_\phi-i[b_h(1/2+ih\partial_\phi),\sin\phi], \tag{8}$$

where $\{\cdots\}$ denotes the anticommutator. Note that the phase-space Hamiltonian (8) is Hermitian; it reduces to the usual nonrigid pendulum form [12,20,22] if one neglects the variation of $b_h(x)$ with respect to x. The non-Hermitian exact Hamiltonian in the Bargmann overcomplete continuous-phase representation was derived in Ref. [21].

The limit of large N of Eq. (5) can be considered by the WKB approach for the discrete Schrödinger equation [11], where the solution of Eq. (5) is written in the form $\Psi=\exp\{iS(x,\tau,h)/h\}$ where $S(x,\tau,h)$ is understood as a series $S=S^{(0)}(x,\tau)+hS^{(1)}(x,\tau)+O(h^2)$ and the terms are assumed to be differentiable functions. In the lowest order one obtains the Hamilton-Jacobi equation for the classical action $S^{(0)}(x,\tau)$,

$$-S_\tau^{(0)}=a(x)-2b_0(x)\cos\left(\frac{\partial S^{(0)}}{\partial x}\right), \tag{9}$$

where $b_0(x)=\sqrt{x(1-x)}$. The classical Hamiltonian thus reads

$$\mathcal{H}=a(x)-2b_0(x)\cos\phi, \tag{10}$$

with the canonical variables $x\in(0,1)$ and $\phi\in(0,2\pi)$: $\{\phi,x\}=1$ (cf. with Ref. [22], where $z=1-2x$). The first-order approximation gives the amplitude: $S^{(1)}=\frac{i}{2}\ln[b_0(x)\sin(S_x^{(0)})]$.

Let us take a slightly different approach. The most important features of the classical dynamics are the stationary points and their stability properties. The classical action can be expanded about a stationary point (say, x_s and ϕ_s)

$$S^{(0)}(x,\tau)=-E^{(cl)}\tau+\phi_s(x-x_s)+O[(x-x_s)^2], \tag{11}$$

where we have used that $S^{(0)}(x,\tau)=-E^{(cl)}\tau+S^{(st)}(x)$ and $\frac{\partial S^{(st)}}{\partial x}(x_s)=\phi_s$. We are interested in the limit of large N. The wave function localized about some x_s point has a singular derivative in the limit $h=1/N\to 0$: $\frac{\partial\Psi}{\partial x}\sim ih^{-1}\phi_s\Psi(x,\tau)$ if $\phi_s\neq 0$. The singularity is due to the classical phase in the wave function. Hence, before taking the limit of large N, we account for the phase explicitly, introducing the transformation (at some x_s point)

$$\Psi(x,\tau)=e^{iN\phi(\tau)(x-x_s)}\psi(x,\tau). \tag{12}$$

On the other hand, the phase $\phi(\tau)$ in Eq. (12) satisfies the evolution equation $\dot{\phi}=\partial H(x_s,\phi)/\partial x$ (obtained by expanding the Schrödinger equation in $x-x_s$ and taking the limit $h\to 0$); hence, it is nothing but the classical phase.

To obtain a reduced Schrödinger equation about a mean-field stationary point we substitute the representation (12) into Eq. (5) and expand the result into series in $\hat{p}$, keeping the terms up to $O(\hat{p}^2)$ (since the derivative is regularized, the expansion is actually in h). As the $O(1)$ term we recover the Hamiltonian (10) as the quantum potential: $\mathcal{V}_0(x)=\mathcal{H}=a(x)-2b_0(x)\cos\phi$. Since the stationary states $\psi(x,\tau)=e^{-iE\tau/h}\psi_E(x)$ correspond to the phase extrema of the quantum potential—i.e., given by $\frac{\partial\mathcal{V}_0(x,\phi)}{\partial\phi}=0$—there are two cases: the positive ($\phi=0$) or negative ($\phi=\pi$) mass of the effective quantum particle (the detailed derivation can be found in Ref. [26]).

III. QUANTUM MODEL ABOUT THE MEAN-FIELD STATIONARY POINTS

The exact Schrödinger equation (5) about the stationary points with $\phi_+=0$ and $\phi_-=\pi$ reduces to

$$ih\partial_\tau\psi=\{\pm\hat{p}\sqrt{x(1-x)}\hat{p}+\mathcal{V}_\pm(x)\}\psi. \tag{13}$$

The upper and lower signs correspond to ϕ_+/ϕ_-, $\mathcal{V}_\pm(x)=\gamma[x^2+(1-x)^2]+\varepsilon x\mp 2\sqrt{x(1-x)}$, and terms of order $O(\hat{p}^3)$ and of order $O(h)$ in the quantum potential and in the coefficients at $\hat{p}$ were neglected. In the usual population imbalance variable $z=1-2x$, Eq. (13) reads

$$ih\partial_\tau\psi=\left\{\mp 2h^2\frac{d}{dz}\sqrt{1-z^2}\frac{d}{dz}+V_\pm(z)\right\}\psi, \tag{14}$$

where the quantum potential simplifies to

$$V_\pm(z)=\frac{1}{2}(\gamma z^2-\varepsilon z)\mp\sqrt{1-z^2}. \tag{15}$$

The symmetry of Eq. (14) with respect to replacing "$\pm$" leads to the following mapping between the repulsive and attractive BEC cases:

$$\gamma_{\mathrm{attr}}=-\gamma_{\mathrm{rep}},\quad z_{\mathrm{attr}}=-z_{\mathrm{rep}},$$

$$\psi_{\mathrm{attr}}(z,\tau;\gamma,\phi_\pm)=\psi_{\mathrm{rep}}^*(-z,\tau;-\gamma,\phi_\mp). \tag{16}$$

Note that it is sufficient to consider also $\varepsilon\geqslant 0$, since $\varepsilon<0$ corresponds to inversion of the coordinate $z\to -z$.

The equivalence (16), however, does not mean that the attractive BEC is similar to the repulsive BEC. As we show below, in both cases the Schrödinger equation (14) with positive mass gives the ground state of BEC and only in the attractive case $V_+(z)$ has the double-well form [see Fig. 1(a) below].

The extrema of the potential (15) solve the equation

$$\gamma\pm\frac{1}{\sqrt{1-z^2}}=\frac{\varepsilon}{2z}. \tag{17}$$

Consider $\gamma>0$ (repulsive BEC), $\varepsilon\geqslant 0$. In the case of positive mass ($\phi=0$) there is just one minimum. For the case of negative mass ($\phi=\pi$) there is a critical γ_{cr} below which there is just one solution which is a minimum of $V=-V_-(z)$, whereas for $\gamma>\gamma_{\mathrm{cr}}$ there are three solutions, two corresponding to local minima and one to a local maximum; see Fig. 1(a). Equation (17) is easily solved graphically by plotting the lhs and rhs as functions of z; see Fig. 1(b). The corre-

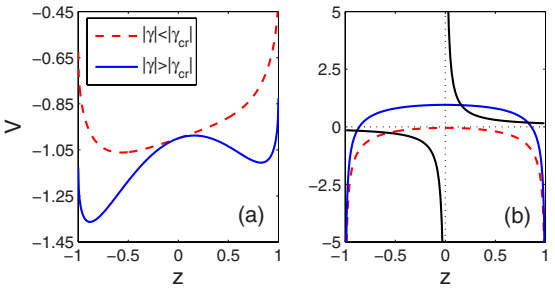

FIG. 1. (Color online) The potential for the effective quantum particle, panel (a) [here $V=-V_{-}(z)$ for the repulsive BEC corresponding to negative mass, $\phi=\pi$, or $V=V_{+}(-z)$ for the attractive BEC for $\phi=0$, positive mass] and the graphical solution for the stationary point, panel (b), where we plot the lhs and rhs of Eq. (17) (again for $\phi=\pi$ for the repulsive BEC, or for $\phi=0$ for the attractive BEC, in the last case the axes are inverted). Here $\varepsilon=0.3$ which gives $|\gamma_{\rm cr}|=1.4521$.

sponding classical phase-space portrait is given in Fig. 2. The critical value of the nonlinearity coefficient reads

$$\gamma_{\rm cr}=\left[1+\left(\frac{\varepsilon}{2}\right)^{2/3}\right]^{3/2}, \tag{18}$$

while the corresponding solution is the point of inflection $z_{\rm cr}=[1+(2/\varepsilon)^{2/3}]^{-1/2}$. For $\gamma>\gamma_{\rm cr}$ two positive solutions bifurcate from it: $z_1<z_{\rm cr}<z_2$, where z_1 is the local maximum of the inverted potential $-V_{-}(z)$. The local maximum solution is an analog of the $z=0$ solution for $\varepsilon\neq 0$.

Finally, all the results obtained for the repulsive BEC are transferred to the attractive BEC case by using the equivalence given in Eq. (16). For instance the cases of $\phi_{\pm}$ are interchanged and the double-well potential of Fig. 1(a) in the case of attractive BEC appears for $\phi=0$ [i.e., now $V=V_{+}(-z)$] and $\gamma<-\gamma_{\rm cr}=-[1+(\frac{\varepsilon}{2})^{2/3}]^{3/2}$.

The stability properties of the stationary points of the classical Hamiltonian are directly related to the quantum potential in Fock space. One can show that the local minima of the quantum potential (or the inverted potential, in the case of negative mass) correspond to the elliptic stationary points of the classical dynamics and the local maximum to a hyperbolic stationary point, which is a physically clear result. In the new variables (see also Ref. [22]),

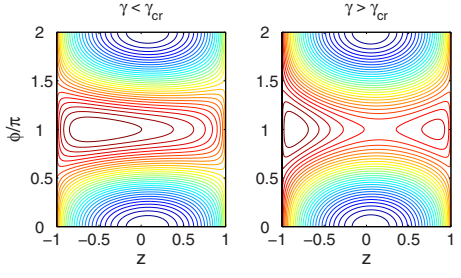

FIG. 2. (Color online) The phase portrait of the classical Hamiltonian, Eq. (19), corresponding to a repulsive BEC in a double-well trap. The parameters are as in Fig. 1.

$$\mathcal{H}=\frac{\gamma}{2}z^2-\frac{\varepsilon}{2}z-\sqrt{1-z^2}\cos\phi, \tag{19}$$

where one must remember that $\{\phi,z\}=-2$. The stationary points of the classical Hamilton equations, $\dot{z}=-2\frac{\partial\mathcal{H}}{\partial\phi}$, $\dot{\phi}=2\frac{\partial\mathcal{H}}{\partial z}$ correspond to the extrema of the quantum potential $V(z)$—i.e., $\cos\phi_s=\pm 1$—whereas z_s is defined from Eq. (17).

IV. GROUND STATE OF BEC IN A DOUBLE-WELL TRAP

To find the ground state of BEC for $N\gg 1$ one needs to compare the zero-point energies at the extremal points (which is the classical energies of the stationary points). We find that the ground state of both repulsive and attractive BEC is given by the effective quantum particle with the positive mass (see more details, Ref. [26]).

The direct link between the classical stationary points and the nature of the corresponding quantum states discussed in Sec. III allows one to get the local approximation for the quantum bound states by directly quantizing the local classical Hamiltonian. Introducing the local phase-space coordinates $\phi=\phi_s+\varphi$ and $z=z_s+\zeta$ in Eq. (19), up to the second-order terms in the local variables we get

$$\mathcal{H}_{\pm}(\zeta,\varphi)=V_{\pm}(z_s)+\frac{1}{2}(a_{\pm}\varphi^2+b_{\pm}\zeta^2), \tag{20}$$

where $a_{\pm}=\sqrt{1-z_s^2}$ and $b_{\pm}=\gamma\pm(1-z_s)^{-3/2}$. The local quantum Hamiltonian is obtained from Eq. (20) by replacing $\varphi\to 2ih\partial_{\zeta}$, since $[\hat{\varphi},\zeta]=2ih$. In the negative-mass case the wave function $\Psi(x,t)$ of BEC in a double-well trap has also the nontrivial phase given by Eq. (12).

Thus, we obtain the local quantum approximation to the classical stationary state of BEC and its energy as follows:

$$\Psi_{\mathcal{E}_{\pm}}(x)=\frac{1}{\pi^{1/4}\sigma_{\pm}^{1/2}}\exp\left\{i\frac{\phi_{\pm}}{h}x-\frac{(x-x_s)^2}{2\sigma_{\pm}^2}\right\},$$

$$\mathcal{E}_{\pm}=V_{\pm}(z_s)+O(h), \tag{21}$$

where $\sigma_{\pm}^2=\frac{1}{2N}\sqrt{\frac{a_{\pm}}{b_{\pm}}}$ is the Gaussian width and we have used that $\Delta z=2\Delta x$. The energy spacing for the few lower levels reads $\Delta\mathcal{E}_{\pm}=h\omega_{\pm}$, where $\omega_{\pm}=2\sqrt{a_{\pm}b_{\pm}}$ is the classical frequency. In the case of negative mass the energy levels of a local quantum Hamiltonian are descending.

A. Properties of the ground state of repulsive BEC

For $\gamma>0$ we obtain the single solution of Eq. (17) corresponding to the positive mass case in the form of a series in ε:

$$z_s=\frac{\varepsilon}{2}(1+\gamma)^{-1}\left[1-\frac{\varepsilon^2}{8(1+\gamma)^3}+O(\varepsilon^4)\right], \tag{22}$$

which is valid for a weakly asymmetric potential $V_{+}(z)$—i.e., $\varepsilon\ll 1+\gamma$. The average atomic population difference between the two wells reads $\langle n_1-n_2\rangle=z_sN$. By the substitution $\gamma\to-\gamma$ and $z_s\to-z_s$ in Eq. (22) we get the position of the

minimum of the inverted potential $-V_-(z)$ in the subcritical case $\gamma < \gamma_{\rm cr}$.

For a weakly asymmetric potential $V_+(z)$ one can also calculate the atom number fluctuations (see the details in Appendix B) using the local approximation for the ground state given by Eq. (21):

$$\langle \Delta n_1^2 \rangle = N^2 \langle (x - x_s)^2 \rangle = \frac{N^2 \sigma_+^2}{2} = \frac{N}{4}(1+\gamma)^{-1/2}\left[1 - \frac{\varepsilon^2(4+\gamma)}{16(1+\gamma)^3} + O(\varepsilon^4)\right], \tag{23}$$

where $x_s = (1 - z_s)/2$.

The result given by Eqs. (21) and (23) can be compared to the exact solution in the noninteracting case ($\varepsilon = 0$), where the Hamiltonian is diagonalized by $c_\pm = (a_1 \pm a_2)/\sqrt{2}$ with the effect $H = -(a_1^\dagger a_2 + a_2^\dagger a_1)/N = (c_-^\dagger c_- - c_+^\dagger c_+)/N$. The eigenstates are given by $(c_+^\dagger)^m (c_-^\dagger)^{N-k}|0,0\rangle$, where $a_1|0,0\rangle = a_2|0,0\rangle = 0$. The ground state corresponds to $m = N$:

$$|\Phi\rangle = \frac{1}{\sqrt{2^N N!}}(a_1^\dagger + a_2^\dagger)^N |0,0\rangle. \tag{24}$$

For large N, approximating the factorial, we get the coherent state in the Fock basis as

$$\Phi(z) = \sqrt{N}\left\langle \frac{1-z}{2}N, \frac{1+z}{2}N | \Phi \right\rangle = \left(\frac{2N}{\pi}\right)^{1/4} \exp\left\{-\frac{N}{4}\left(z^2 + \frac{z^4}{6} + \cdots\right)\right\}, \tag{25}$$

which coincides with the approximate solution (21) up to the $O(z^4)$ term in the exponent.

Equations (21)–(23) capture all three known regimes of repulsive BEC tunneling in the double-well trap (see, for instance, Refs. [12,13,25]): (i) Rabi regime, when the coherence is very high and the atom number fluctuations are large (essentially the interaction free regime), $\gamma \ll 1$; (ii) Josephson regime, when the coherence is high and the atom number fluctuations are small, $1 \ll \gamma \ll N^2$; and (iii) Fock regime, when the coherence is low and the atom number fluctuations vanish, $\gamma \gg N^2$.

B. Transformation of the ground state of attractive BEC

Subcritical γ. In the case $|\gamma| < \gamma_{\rm cr}$ the ground state of attractive BEC is also given by the general result (21) for the positive-mass case (i.e., the upper sign). The average population difference is again given by the series solution (22) and the number fluctuations are given by the same formula (23) as in the repulsive case. However, since now $\gamma < 0$, there is an essential difference: even moderate attractive interactions strongly enhance the atom number fluctuations (which fact leads to the absence of the Josephson regime for attractive BEC).

For γ approaching (from above) the critical value $-\gamma_{\rm cr}$ the fluctuations given by the local oscillator approximation (21) diverge, which is easily seen from Eq. (23) applied to the case $\varepsilon = 0$. In the general case the result is similar and follows from the exact expression for σ_+^2 with the use of the exact value for the point of inflection z_s [given below Eq. (18) in Sec. III] and the expression $\gamma_{\rm cr} = (1 - z_{\rm cr}^2)^{-3/2}$.[2] The divergence results from the oscillator approximation of the wave function $\Psi(x)$, Eq. (21), which breaks down at the critical value of γ, since at this point the potential is quartic (we give the case $\varepsilon = 0$ and $z_s = 0$ for simplicity):

$$V_+(z) = -\frac{z^2}{2} - \sqrt{1 - z^2} = \frac{z^4}{8} + \frac{z^6}{16} + \cdots, \tag{26}$$

Supercritical γ. In the case of $|\gamma| > \gamma_{\rm cr}$, for γ such that the potential $V_+(z)$ is a double well with well-separated wells (the form of this potential is essentially determined by the atomic interaction parameter), the oscillator approximation is still valid locally [i.e., about the two minima of the potential $V_+(z)$; see Fig. 1] and the ground state can be now approximated by a linear combination of the local eigenfunctions.

The case $\varepsilon = 0$ is the most interesting. The two local minima, solutions of Eq. (17), read $z_s^{(\pm)} = \pm\sqrt{1 - \gamma^{-2}}$. The validity of the local approximation by oscillator eigenfunctions in the two wells is the width of the local eigenfunctions being much smaller than the distance between the two wells. We have $z_R - z_L = 2\sqrt{1 - \gamma^{-2}}$ and using Eq. (21) $\langle (z - z_L)^2 \rangle = 4\langle (x - x_L)^2 \rangle = N^{-1}|\gamma|^{-1}(\gamma^2 - 1)^{-1/2}$. Therefore, the applicability condition $\langle (z - z_L)^2 \rangle \ll (z_R - z_L)^2/4$ reads

$$|\gamma|(|\gamma| - |\gamma|^{-1})^3 \gg \frac{1}{N^2}, \tag{27}$$

where on the lhs we have a monotonically growing function of $|\gamma|$. The condition is satisfied for $|\gamma|$ slightly above the critical value $|\gamma| = 1$; e.g., setting $|\gamma| = 1 + \delta$ with $\delta \ll 1$ in Eq. (27), we obtain $\delta \gg N^{-2/3}$, which for $N = 1000$ gives $\delta \gg 0.01$.

To obtain the ground state we need to evaluate the tunneling rate—i.e., the matrix element $\langle \Psi_L | \hat{H} | \Psi_R \rangle$, where one can use the local approximation (21) and $\hat{H}$ can be taken from Eq. (14). We have (here $s = L, R$)

$$\Psi_s(z) = \frac{1}{\pi^{1/4}\sqrt{\sigma}} e^{-(z - z_s)^2/2\sigma^2}, \tag{28}$$

where $\sigma^2 = 4\sigma_+^2 = \frac{2}{N}|\gamma|^{-1}(\gamma^2 - 1)^{-1/2}$. There is an exponentially small overlap between Ψ_L and Ψ_R:

$$\langle \Psi_L | \Psi_R \rangle = \frac{1}{\sqrt{\pi}\sigma}\int_{-1}^{1} dz \exp\left\{-\frac{(z - z_L)^2 + (z - z_R)^2}{2\sigma^2}\right\} = \exp\left\{-\frac{N}{2}|\gamma|^{-1}(\gamma^2 - 1)^{3/2}\right\}, \tag{29}$$

where we have used that $(z - z_L)^2 + (z - z_R)^2 = 2(z^2 + z_L^2)$ and the normalization of the function $\Psi(z) = \pi^{-1/4}\sigma^{-1/2}\exp\{-\frac{z^2}{2\sigma^2}\}$. Using the integration by parts we get

[2] Note that Eq. (23) seems to give a higher value $\gamma = -1$ than $-\gamma_{\rm cr}$ for divergence of the fluctuations for $\varepsilon \neq 0$. However, by more careful inspection one notices that the second term in the square brackets for the number fluctuations becomes of order 1 at the critical γ; this is an artifact of the approximation in Eq. (22).

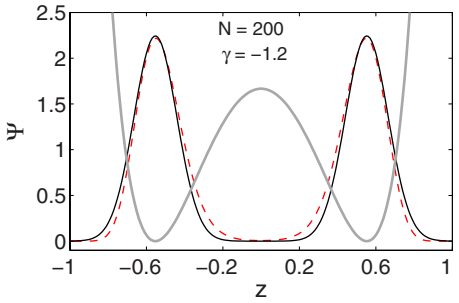

FIG. 3. (Color online) The ground state of attractive BEC in the supercritical case: analytical [given by Eqs. (28) and (32), solid line] vs numerical diagonalization of the Hamiltonian (dashed line). The thick gray line shows schematically the effective potential $V_+(z)$. Here $N=200$, $\gamma=-1.2$, and $\varepsilon=0$.

$$\langle\Psi_L|\hat{H}|\Psi_R\rangle = \frac{2}{\sigma^4 N^2}\langle\Psi_L|(z-z_L)(z-z_R)\sqrt{1-z^2}|\Psi_R\rangle + \langle\Psi_L|\gamma z^2/2 - \sqrt{1-z^2}|\Psi_R\rangle.$$

To estimate the products we use $(z-z_L)(z-z_R)=z^2-1+\gamma^{-2}$ and set $z=0$ where the overlap of the wave functions $\Psi_{L,R}(z)$ is maximal, with the effect

$$\langle\Psi_L|\hat{H}|\Psi_R\rangle \approx -\left[1+\frac{(\gamma^2-1)^2}{2}\right]\langle\Psi_L|\Psi_R\rangle. \tag{30}$$

It is natural to define the "tunneling coefficient" κ for the effective quantum particle as follows [cf. with Eq. (2)]:

$$\kappa = -\langle\Psi_L|\hat{H}|\Psi_R\rangle \approx \left[1+\frac{(\gamma^2-1)^2}{2}\right]\exp\left\{-\frac{N}{2|\gamma|}(\gamma^2-1)^{3/2}\right\}. \tag{31}$$

The ground and first excited states in the supercritical double-well potential $V_+(z)$ for $\gamma<0$ read

$$|G\rangle = \frac{1}{\sqrt{2}}(|\Psi_L\rangle + |\Psi_R\rangle), \quad |E\rangle = \frac{1}{\sqrt{2}}(|\Psi_L\rangle - |\Psi_R\rangle), \tag{32}$$

where $\Psi_{L,R}(z)$ are given by Eq. (28).

The analytical expression for the ground state, Eq. (32), is a very good approximation of the exact ground state of the quantum Hamiltonian (1); see Fig. 3. On the other hand, the extremely small degenerate level energy splitting, given by $\delta\mathcal{E}=2\kappa$ and defined by the tail slope of the solution at $z=0$, is only a qualitative result. The energy splitting is usually estimated by perturbation theory, but this is valid only for small values of N (since the small parameter is equivalent to N/γ; see, for details, Ref. [27]).

For large $|\gamma|$ above the critical value the ground state of the attractive BEC in the symmetric double-well trap is the Schrödinger cat state, i.e., a superposition of two macroscopicaly occupied states (see also Refs. [28,29]). Precisely, for $|\gamma| \gg \sqrt{N}$ we have

$$|G\rangle = \frac{1}{\sqrt{2}}(|N,0\rangle + |0,N\rangle). \tag{33}$$

Indeed, in the supercritical case $\Psi_{L,R}(z)$, Eq. (28), has the Fock-space width given by $N\sqrt{\langle(z-z_s)^2\rangle}/2=\frac{\sqrt{N}}{2}|\gamma|^{-1/2}(\gamma^2-1)^{-1/4}\approx\sqrt{N}/(2|\gamma|)\ll 1$ for $|\gamma|\gg\sqrt{N}$.

V. MQST AND THE NEGATIVE-MASS QUANTUM PARTICLE

The equivalence between the repulsive and attractive BEC cases, given by Eq. (16), means that the repulsive BEC also contains the Schrödinger cat state (see also Ref. [30]), which is an excited stationary state. The double-well potential $V=V_-(z)$ for the classical phase $\phi=\pi$ is responsible for the MQST states of a repulsive BEC in the symmetric double-well trap, predicted in Ref. [22] and observed experimentally in Ref. [14]. There are two major types of MQST: the phase-locked ($\phi\approx\pi$) states and the running-phase states ($\phi\propto t$).

Consider the symmetric double-well trap ($\varepsilon=0$). Following the arguments of Ref. [22]—i.e., using the energy E conservation and Eq. (19)—one obtains

$$\frac{1}{4}\left(\frac{dz}{d\tau}\right)^2 = 1-z^2-\left(\frac{\gamma}{2}z^2-E\right)^2. \tag{34}$$

Equation (34) results in a neighborhood of $z=0$ being inaccessible if $|E|>1$. On the other hand, for $N\gg 1$ the energy satisfies $V_+(z)\leqslant E\leqslant V_-(z)$ and the above is possible only when the potential $V_-(z)=\frac{\gamma}{2}z^2+\sqrt{1-z^2}$ is an inverted double well and the energy line crosses the central (inverted) barrier. Hence, MQST is possible only for $\gamma>1$. On the other hand, the mean-field condition for MQST reads $\gamma>\gamma_c$, where [22]

$$\gamma_c = 2\frac{1+\sqrt{1-z^2(0)}\cos[\phi(0)]}{z^2(0)}. \tag{35}$$

The mean-field critical value always satisfies $\gamma_c>1$. [This is easily seen by rewriting Eq. (35) as $\gamma z^2/2=1+\sqrt{1-z^2}\cos\phi$ and noticing that if $\gamma\leqslant 1$ the functions on the lhs and rhs have no intersections for $0<|z|<1$.]

Equation (35) gives $\gamma_c\geqslant 2$ for $\cos\phi(0)\geqslant 0$. For $\gamma>2$ the MQST condition reads $|z(0)|>z_c$, where z_c is the solution of Eq. (35). On the other hand, for $\cos\phi(0)<0$ and $1+|\sin\phi(0)|<\gamma<2$ there is an interval of the initial population imbalance for MQST: $z_1<|z(0)|<z_2$, where $z_{1,2}$ solve Eq. (35) (see also Ref. [22]).

If repulsive BEC is prepared in one well of the double-well trap and the initial phase $\phi(0)\approx\pi$, one can use the negative-mass Schrödinger equation (14) to explain the quantum dynamics. In this case the inverse quantum potential $V=-V_-(z)$ in Fock space has double-well form with quasidegenerate energy levels, which reflect the existence of two classical fixed points $z_s^{(\pm)}=\pm\sqrt{1-\gamma^{-2}}$. The degeneracy is estimated as twice the tunneling coefficient of Eq. (31). Therefore, experimental observation of phase-locked mean-field MQST ($\langle\phi\rangle\approx\pi$) is subject to the quantum condition that the oscillation time of the effective quantum particle in one of the wells be much less than the tunneling time be-

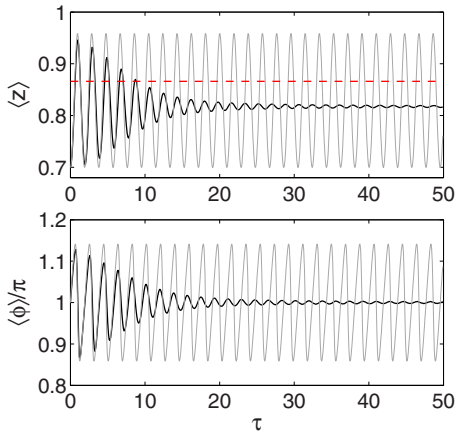

FIG. 4. (Color online) The phase-locked MQST state dynamics: quantum averages (black lines), as defined by Eq. (37), vs classical dynamics (gray lines). The dashed line in the upper panel gives the classical stationary point $z_s=0.866$. Here $N=1000$, $\gamma=2$ (whereas $\gamma_c=1.23$), and $\varepsilon=0$. The initial Gaussian distribution of width $\Delta z=0.12$ centered at the point $\langle z\rangle=0.78$ and with phase $\phi=\pi$ was used.

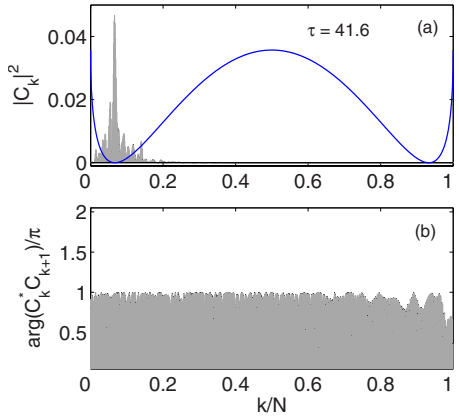

FIG. 5. (Color online) The snapshot of the atomic number distribution (a) (represented by vertical bars) of the phase-locked MQST state and that of the distributed quantum phase (b) (given by bars). The line in panel (a) gives a schematic portrait of the inverse quantum potential $-V_-(1-2k/N)$.

tween the wells of the double-well potential $V_-(z)$, which is almost always satisfied due to the extremely small degeneracy $\delta\mathcal{E}=2\kappa\ll 1$ (recall that $\delta\mathcal{E}$, the degeneracy in Fock space, is measured in units of the real-space double-well energy level degeneracy δE). Indeed, we have to show that $\delta\mathcal{E}\ll h\omega_-=2h\sqrt{a_-b_-}$, or using the estimate (31),

$$\left[1+\frac{(\gamma^2-1)^2}{2}\right]\exp\left\{-\frac{N}{2\gamma}(\gamma^2-1)^{3/2}\right\}\ll\frac{\sqrt{\gamma^2-1}}{N}, \tag{36}$$

which is satisfied for all γ just above the critical value, even for a small number of BEC atoms. This fact makes possible the experimental observation of phase-locked mean-field MQST. A similar conclusion was made before using a different approach [31,32]. We note also that the π-phase MQST was analyzed in Ref. [31] by considering the numerical eigenvalue spectrum and was related to the appearance of the quasidegenerate energy doublets.

Numerical simulations show that the quantum average values, defined as[3]

$$\langle z\rangle=1-\frac{2}{N}\sum_{k=0}^{N}k|C_k|^2,\quad \langle\phi\rangle=\arg\langle e^{i\hat{p}}\rangle=\arg\sum_{k=0}^{N-1}C_k^*C_{k+1}, \tag{37}$$

initially follow the mean-field dynamics; see Fig. 4. The numerical method of propagating the Schrödinger equation is adopted from Ref. [33] (see also Ref. [10]).

[3]The usual definition of the phase is via the average $\langle a_1^\dagger a_2\rangle$. Our definition is slightly different and prompted by the quantum-classical correspondence established in Sec. II: $\hat{p}\to\phi$. The two definitions agree very well for large N. We use $e^{i\hat{p}}$ to define the dispersion, since the shift operator is defined for any N, while $\hat{p}$ is ill defined for small N.

During the evolution, the atomic distribution in Fock space remains localized in one of the wells of the inverse quantum potential $V=-V_-(z)$, Fig. 5(a). The distributed quantum phase ϕ_k, defined as $\phi_k=\arg(C_k^*C_{k+1})$, remains very close to π; see Fig. 5(b). For longer times the classical oscillations are subject to collapses and revivals [5].

To get a quantitative estimate of the validity the classical dynamics, one can use the standard deviations of the quantum variables, defined as $\Delta z=2\Delta x=2[\langle(x-\langle x\rangle)^2\rangle]^{1/2}$ and

$$\Delta e^{i\hat{p}}=[\langle(e^{-i\hat{p}}-\langle e^{-i\hat{p}}\rangle)(e^{i\hat{p}}-\langle e^{i\hat{p}}\rangle)\rangle]^{1/2}=[1-|\langle e^{i\hat{p}}\rangle|^2]^{1/2} \tag{38}$$

(we assume that $|\langle N,0|\Psi\rangle|=0$; in the case of $|\langle N,0|\Psi\rangle|\neq 0$ and $|\langle 0,N|\Psi\rangle|=0$, one can use the operator $e^{-i\hat{p}}$ instead with similar result). From Eq. (38) one concludes that for the average phase defined in Eq. (37) we have $\langle e^{i\hat{p}}\rangle=\alpha e^{i\langle\phi\rangle}$ with some $\alpha\leqslant 1$. One can also show that

$$\Delta e^{i\hat{p}}=(\Delta^2\cos\hat{p}+\Delta^2\sin\hat{p})^{1/2}; \tag{39}$$

hence, for a small deviation, $\Delta e^{i\hat{p}}\approx\Delta\hat{p}$—i.e., $\Delta\phi$. Using the Schwartz inequality $\Delta A\Delta B\geqslant\frac{1}{2}\langle[A,B]\rangle|$ for $A=e^{i\hat{p}}$ and $B=z$ we arrive at

$$\Delta\Omega\equiv\frac{\Delta e^{i\hat{p}}}{|\langle e^{i\hat{p}}\rangle|}\Delta z\geqslant h. \tag{40}$$

The quantity $\Delta\Omega$ characterizes the quantum-state proximity to the semiclassical state.

For the simulations presented in Fig. 4, the standard deviation Δz decreases from 0.122 to 0.096, while $\Delta e^{i\hat{p}}$ grows from 0.0479 to 0.268 (the average $|\langle e^{i\hat{p}}\rangle|$ decreases from 0.999 to 0.963). In this case the quantity $\Delta\Omega$, Eq. (40), grows during the evolution by one order of magnitude as compared to the initial value on the order of $h=1/N$.

In the experiment of Ref. [14] the running-phase MQST was observed. Its classical dynamics is well understood [22]. Here, we focus on the full quantum dynamics. First of all we have found that the quantum averages over the MQST state

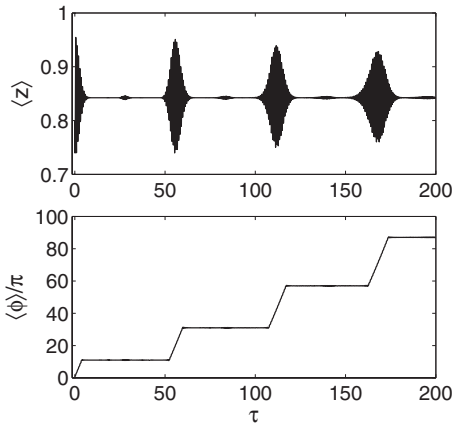

FIG. 6. The quantum collapses and revivals of the running-phase MQST state. We use $N=200$, $\gamma=5$, and $\varepsilon=0$. The initial condition is a Gaussian with $\langle z\rangle=0.8$, $\langle\phi\rangle=0.75\pi$ (thus $\gamma_c=1.8$) and width $\sigma=0.05N$. We show the quantum average $\langle z\rangle$ (upper panel) and the average phase $\langle\phi\rangle$, (lower panel) as defined by Eq. (37).

with the running phase, though initially follow the classical dynamics, are subject to quantum collapses and revivals; see Fig. 6. In particular, the dynamics of the quantum average $\langle\phi\rangle$ is interrupted by plateaus of constant phase, while the classical phase follows almost linear growth.

Moreover and most importantly, the first occurrence of the quantum collapse of the running phase (see Fig. 7) is accompanied by a rapid growth (the peaks in the inset of the lower panel of Fig. 7) of the quantity $\Delta\Omega$ (40) (initially $\Delta\Omega\approx h$). The quantum dispersions grow exponentially, and the dispersion of the phase (i.e., $\Delta e^{i\hat{\phi}}$) reaches its maximal value close to the absolute maximum (equal to 1) at the first collapse (and at each subsequent collapse); see Fig. 8. The dispersions decrease (though not reaching the initial value) at the revivals of the classical dynamics of the quantum averages. Note that, notwithstanding the difference between the classical and

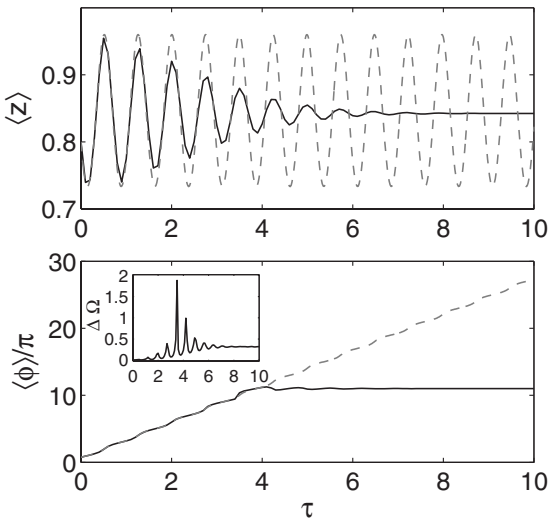

FIG. 7. The classical dynamics (dashed lines) and the corresponding quantum averages (solid lines) at the first occurrence of quantum collapse of the running-phase MQST state of Fig. 6. In the inset in the lower panel we give the quantity $\Delta\Omega$ (40).

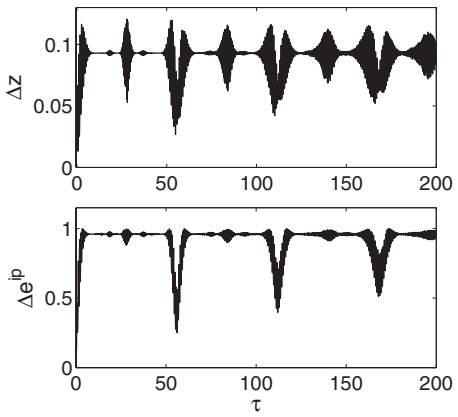

FIG. 8. The dispersions of the quantum distributions of z and $e^{i\hat{\phi}}$ for longer times corresponding to Figs. 6 and 7.

quantum dynamics (the collapses and revivals), the population imbalance z effectively remains "trapped" during the evolution, since the quantum dispersion Δz is significantly smaller than the population imbalance itself.

We found that the occurrence of the first collapse depends on the initial state (for instance, the dispersions of the number of atoms and the quantum phase), but does not seem to depend on the number of atoms for a fixed initial state [e.g., for a fixed average and dispersion of the observable $(n_1-n_2)/N$], while the subsequent quantum revivals and collapses do depend on N: we have found no revivals for $N=1000$ and the other parameters of Fig. 6 up to $\tau=200$. The clean visibility of the collapses and revivals (as in Fig. 6) depends on the value of $\Delta\Omega$ corresponding to the initial state: the closer is the state to classical—i.e., the closer is $\Delta\Omega$ to the lower limit $1/N$—the more pronounced are the subsequent collapses and revivals.

Next, let us demonstrate that experimental observation of at least the first occurrence of the quantum collapse of the running phase is possible already with the setup of Ref. [14]. Though the exact initial quantum state of the experiment on MQST is not known, we can try to reproduce the dynamics using the experimental values on the initial number of atoms, $N=1150\pm150$, quantum averages $\langle z\rangle=0.062$, $\langle\phi\rangle=0$, and dispersion $\Delta z=0.06$ by modeling the initial state by a Gaussian [in Fock space; see Eq. (21)] fitting it to the above values. Both the method of creating the initial population imbalance of Ref. [14] by using an initially highly asymmetric trap with the subsequent sudden ramp to a symmetric trap and the results of Sec. IV A indicate that a Gaussian is indeed a good approximation of the initial state. First of all, we have reproduced the Josephson oscillations similar to Fig. 2(a) of Ref. [14] (with all the features resembling the experimental results), to make sure that we are reproducing the experimental regime. This also allows to estimate the time unit (though very imprecisely) $t=t_{\mathrm{expt}}\tau$ with $t_{\mathrm{expt}}\sim30-40$ ms. The MQST dynamics for the experimental initial conditions is presented in Fig. 9 [compare with Fig. 2(b) of Ref. [14]].

Note that the collapse of the running phase in Fig. 9 occurs about $\phi(\tau)=3\pi$, which is close to the final phase of the experiment [14] when the phase fluctuations take over. The

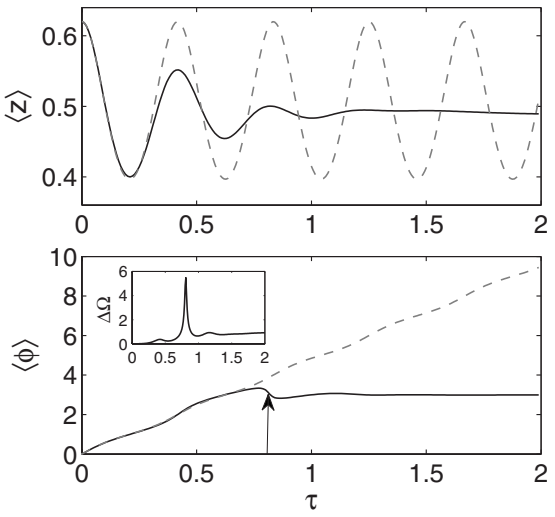

FIG. 9. The quantum dynamics of the running-phase MQST state for $N=1150$, $\gamma=15$, and the initial values $\langle z\rangle=0.62$ and $\langle\phi\rangle=0$. The initial state is Gaussian with the width fitted to reproduce the experimental standard deviation $\Delta z=0.06$. In the inset of the lower panel we give $\Delta\Omega$, Eq. (40). The arrow indicates the time of occurrence of the peak shown in the inset.

exponential growth of $\Delta e^{i\hat{p}}$—i.e., of the fluctuations of the quantum phase variable (see Fig. 10)—is similar as for the case of $\langle\phi\rangle=0.75\pi$ (Fig. 8), with reaching a maximum (close to the absolute one equal to 1) at the time of the quantum collapse of the running phase. We have not found subsequent revivals up to $\tau=200$, similar as for the large number of atoms ($N=1000$) in the case of the initial phase $\langle\phi\rangle=0.75\pi$; however, for a smaller number of atoms (for instance, $N=200$), they are present at longer times.

Concluding this section, our principal results are that running-phase MQST is subject to quantum collapses and revivals and that the first quantum collapse is associated with an exponential growth of the quantum fluctuations of the phase distribution; see Figs. 8 and 10, reaching a maximal value at the collapse time. In this case, $\Delta\Omega$, Eq. (40), rapidly grows (by two or three orders of magnitude; the absolute value of the phase exponent $\alpha=|\langle e^{i\hat{p}}\rangle|$ rapidly decreases) and reaches a peak value at the first collapse. Here we note that the growing fluctuations are also seen in the experimental results on the running-phase MQST presented in Ref. [14]. The experimental results also contain finite-temperature effects. However, finite-temperature effects being negligible, the quantum evolution on its own rapidly destroys the mean-field running phase of the MQST state by an exponential growth of the quantum phase dispersion in an experimentally feasible time (and within the experimental time range there is no subsequent revival). Although the population imbalance stays trapped (due to the small dispersion of the corresponding quantum observable), the real MQST is not the mean-field effect, but has essentially quantum character.

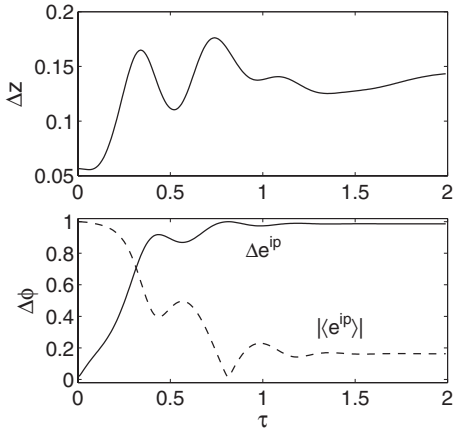

FIG. 10. The dispersions of the quantum distributions of z (upper panel) and $e^{i\hat{p}}$ (lower panel) corresponding to Fig. 9. In the lower panel $\alpha=|\langle e^{i\hat{p}}\rangle|$ is also given (dashed line).

VI. CONCLUSIONS

We have proposed an analytical approach for a description of quantum phenomena in systems of a large number of interacting bosons occupying only a few modes (two in the present study). The method links the many-boson system with the dynamics of a single quantum particle in a potential, where the normalized occupation number in Fock space serves as the particle coordinate. We have used as the example the well-known two-mode model, describing, for instance, BEC tunneling in a double-well trap—i.e. the boson Josephson effect. Our method has allowed us to (a) analyze the quantum states corresponding to the mean-field stationary points, (b) study the transformation of the ground state of the system of identical bosons for attractive and repulsive interactions, (c) derive the quantum fluctuations of the number of atoms in the ground state, (d) relate the appearance of the macroscopic quantum self-trapping phenomenon to the double-well shape of the potential for the effective quantum particle, and (e) explain the quantum nature of the phase-locked and running-phase mean-field self-trapping of BEC in the double-well potential.

For the running-phase macroscopic self-trapping phenomenon of BEC, which is a feature of the mean-field approach, we have found that even in the absence of finite-temperature effects, the quantum evolution on its own destroys the classical running phase of the mean-field MQST dynamics. It happens due to a quantum collapse caused by an exponential growth of the quantum phase dispersion. We estimate that it occurs in an experimentally feasible time and the subsequent revival does not. The population imbalance trapping is due to the small dispersion of the corresponding quantum observable; however, the real MQST state is not the mean-field one (which has the lhs of the Heisenberg uncertainty relation—i.e., the product of dispersions of the relative particle number and the phase, on the order of N^{-1}), but a more complicated *essentially quantum* state with an undefined relative phase (which has product of dispersions of the relative particle number and the phase much larger than N^{-1}).

Finally, our approach is of a general nature and can be applied to other boson models including the theory of molecular-atomic coherence in BEC with the account of the nonlinear interactions [34], the quantum model of nonlinear intraband tunneling of BEC in optical lattices [9,10], and many others.

ACKNOWLEDGMENTS

V.S.S. acknowledges support by FAPESP of Brazil (Grant No. 2008/01150-8) and thanks A. F. R. de Toledo Piza, E. J. V. de Passos, and M. O. C. Pires for invaluable discussions. M.T. acknowledges support by Polish Government scientific funds (2007–2010).

APPENDIX A: THE FULL TWO-MODE BOSON JOSEPHSON MODEL

One can show that the full two-mode boson model describing BEC in a double-well trap can be cast in the (dimensional) form

$$H = \delta V a_1^\dagger a_1 - [J_{\rm lin} + J_{\rm nonl}(N-1)](a_1^\dagger a_2 + a_2^\dagger a_1) + \frac{\rho_1 - \rho_2}{2}[(a_1^\dagger a_1)^2 + (a_2^\dagger a_2)^2] + \frac{\rho_2}{2}(a_1^\dagger a_2 + a_2^\dagger a_1)^2, \tag{A1}$$

where some scalar N-dependent term has been discarded. The coefficients are given as $J_{\rm lin} = \delta E/2$,

$$J_{\rm nonl} = -g\int d^3\mathbf{x}\,\varphi_\alpha(\mathbf{x})\varphi_\beta^3(\mathbf{x}),$$

$$\rho_1 = g\int d^3\mathbf{x}\varphi_\alpha^4(\mathbf{x}),$$

$$\rho_2 = g\int d^3\mathbf{x}\,\varphi_\alpha^2(\mathbf{x})\varphi_\beta^2(\mathbf{x}) \tag{A2}$$

(the subscripts α and β are permutation of the list $\{L,R\}$ and the functions give the localized states in the left or right well defined by the appropriate linear combinations of the ground state and the first exited state; see Sec. II). The derivation is similar to that of Refs. [23,13] and is omitted. However, with the help of numerical evaluation, one can verify that for all double-well traps with two lower degenerate levels E_1 and E_2 satisfying the inequality $\delta E = E_2 - E_1 \ll E_3 - E_2$ the coefficients satisfy

$$\rho_1 \gg \rho_2 \gg |J_{\rm nonl}|. \tag{A3}$$

The coefficients $J_{\rm lin}$ and $J_{\rm nonl}(N-1)$, however, can be of the same order. Discarding the small terms and dividing the Hamiltonian by the quantity $[J_{\rm lin}+J_{\rm nonl}(N-1)]N$ one gets the reduced model given by Eq. (1) with a different definition of the parameters.

APPENDIX B: THE RELATIVE ATOM NUMBER FLUCTUATIONS IN THE POSITIVE-MASS CASE

We have $\langle (x-x_s)^2\rangle = \sigma_+^2/2$, where

$$\sigma_+^2 = \frac{1}{2N}\left[\frac{(1-z_s)^{1/2}}{\gamma + (1-z_s^2)^{-3/2}}\right]^{1/2}. \tag{B1}$$

From Eq. (17) for positive-mass case we get $(1-z_s^2)^{1/2} = \frac{\varepsilon}{2z_s} - \gamma$. Now using Eq. (22) we obtain

$$\frac{\varepsilon}{2z_s} - \gamma = 1 + \frac{\varepsilon^2}{8(1+\gamma)^2} + O(\varepsilon^4),$$

$$\gamma + \left(\frac{\varepsilon}{2z_s} - \gamma\right)^3 = (1+\gamma)\left[1 + \frac{3\varepsilon^2}{8(1+\gamma)^3} + O(\varepsilon^4)\right].$$

Therefore

$$\sigma_+^2 = \frac{1}{2N}(1+\gamma)^{-1/2}\left[1 - \frac{\varepsilon^2(4+\gamma)}{16(1+\gamma)^3} + O(\varepsilon^4)\right]. \tag{B2}$$

[1] N. N. Bogoliubov and N. N. Bogoliubov, Jr., *Introduction to Quantum Statistical Mechanics* (World Scientific, Singapore, 1982).
[2] L. P. Pitaevskii and S. Stringari, *Bose-Einstein Condensates in Gases* (Cambridge University Press, Cambridge, England, 2003).
[3] Y. Castin and R. Dum, Phys. Rev. A **57**, 3008 (1998).
[4] S. Aubry, S. Flach, K. Kladko, and E. Olbrich, Phys. Rev. Lett. **76**, 1607 (1996).
[5] G. J. Milburn, J. Corney, E. M. Wright, and D. F. Walls, Phys. Rev. A **55**, 4318 (1997).
[6] A. Vardi and J. R. Anglin, Phys. Rev. Lett. **86**, 568 (2001).
[7] J. R. Anglin and A. Vardi, Phys. Rev. A **64**, 013605 (2001).
[8] K. W. Mahmud, H. Perry, and W. P. Reinhardt, Phys. Rev. A **71**, 023615 (2005).
[9] V. S. Shchesnovich and V. V. Konotop, Phys. Rev. A **75**, 063628 (2007).
[10] V. S. Shchesnovich and V. V. Konotop, Phys. Rev. A **77**, 013614 (2008).
[11] P. A. Braun, Rev. Mod. Phys. **65**, 115 (1993).
[12] A. J. Leggett, Rev. Mod. Phys. **73**, 307 (2001).
[13] R. Gati and M. K. Oberthaler, J. Phys. B **40**, R61 (2007).
[14] M. Albiez, R. Gati, J. Fölling, S. Hunsmann, M. Cristiani, and M. K. Oberthaler, Phys. Rev. Lett. **95**, 010402 (2005).
[15] Y. Shin, M. Saba, T. A. Pasquini, W. Ketterle, D. E. Pritchard, and A. E. Leanhardt, Phys. Rev. Lett. **92**, 050405 (2004).
[16] C. Lee, Phys. Rev. Lett. **97**, 150402 (2006).
[17] M. Jääskeläinen and P. Meystre, Phys. Rev. A **73**, 013602 (2006).
[18] B. V. Hall, S. Whitlock, R. Anderson, P. Hannaford, and A. I. Sidorov, Phys. Rev. Lett. **98**, 030402 (2007).
[19] G.-B. Jo, Y. Shin, S. Will, T. A. Pasquini, M. Saba, W. Ketterle, D. E. Pritchard, M. Vengalattore, and M. Prentiss, Phys. Rev. Lett. **98**, 030407 (2007).
[20] L. Pitaevskii and S. Stringari, Phys. Rev. Lett. **87**, 180402 (2001).
[21] J. R. Anglin, P. Drummond, and A. Smerzi, Phys. Rev. A **64**, 063605 (2001).
[22] A. Smerzi, S. Fantoni, S. Giovanazzi, and S. R. Shenoy, Phys. Rev. Lett. **79**, 4950 (1997); S. Raghavan, A. Smerzi, S. Fan-

toni, and S. R. Shenoy, Phys. Rev. A **59**, 620 (1999).
[23] D. Ananikian and T. Bergeman, Phys. Rev. A **73**, 013604 (2006).
[24] V. S. Shchesnovich, S. B. Cavalcanti, and R. A. Kraenkel, Phys. Rev. A **69**, 033609 (2004).
[25] G.-S. Paraoanu, S. Kohler, F. Sols, and A. J. Leggett, J. Phys. B **34**, 4689 (2001).
[26] V. S. Shchesnovich and M. Trippenbach, e-print arXiv:0804.0234.
[27] L. Bernstein, J. C. Eilbeck, and A. C. Scott, Nonlinearity **3**, 293 (1990).
[28] Y. Zhou, H. Zhai, R. Lü, Zh. Xu, and L. Chang, Phys. Rev. A **67**, 043606 (2003).
[29] T.-L. Ho and C. V. Ciobanu, J. Low Temp. Phys. **125**, 257 (2004).
[30] R. Gati, J. Esteve, B. Hemmerling, T. B. Ottenstein, J. Appmeier, A. Weller, and M. K. Oberthaler, New J. Phys. **8**, 189 (2006).
[31] A. N. Salgueiro, A. F. R. de Toledo Piza, G. B. Lemos, R. Drumond, M. C. Nemes, and M. Weidemüller, Eur. Phys. J. D **44**, 537 (2007).
[32] S. Raghavan, A. Smerzi, and V. M. Kenkre, Phys. Rev. A **60**, R1787 (1999).
[33] H. Tal-Ezer and R. Kosloff, J. Chem. Phys. **81**, 3967 (1984).
[34] M. Kostrun, M. Mackie, R. Côté, and J. Javanainen, Phys. Rev. A **62**, 063616 (2000); J. Calsamiglia, M. Mackie, and K.-A. Suominen, Phys. Rev. Lett. **87**, 160403 (2001).
[35] L. Susskind and J. Glogower, Physics (Long Island City, N.Y.) **1**, 49 (1964).